

## Identification of the $\gamma$ Subunit-interacting Residues on Photoreceptor cGMP Phosphodiesterase, PDE6 $\alpha'$ \*

Received for publication, September 5, 2000, and in revised form, September 28, 2000  
Published, JBC Papers in Press, October 6, 2000, DOI 10.1074/jbc.M008094200

Alexey E. Granovsky and Nikolai O. Artemyev‡

From the Department of Physiology and Biophysics, University of Iowa College of Medicine, Iowa City, Iowa 52242

**Photoreceptor cGMP phosphodiesterase (PDE6) is the effector enzyme in the G protein-mediated visual transduction cascade. In the dark, the activity of PDE6 is shut off by the inhibitory  $\gamma$  subunit ( $P\gamma$ ). Chimeric proteins between cone PDE6 $\alpha'$  and cGMP-binding and cGMP-specific PDE (PDE5) have been constructed and expressed in Sf9 cells to study the mechanism of inhibition of PDE6 catalytic activity by  $P\gamma$ . Substitution of the segment PDE5-(773–820) by the corresponding PDE6 $\alpha'$ -(737–784) sequence in the wild-type PDE5 or in a PDE5/PDE6 $\alpha'$  chimera containing the catalytic domain of PDE5 results in chimeric enzymes capable of inhibitory interaction with  $P\gamma$ . The catalytic properties of the chimeric PDEs remained similar to those of PDE5. Ala-scanning mutational analysis of the  $P\gamma$ -binding region, PDE6 $\alpha'$ -(750–760), revealed PDE6 $\alpha'$  residues essential for the interaction. The M758A mutation markedly impaired and the Q752A mutation moderately impaired the inhibition of chimeric PDE by  $P\gamma$ . The analysis of the catalytic properties of mutant PDEs and a model of the PDE6 catalytic domain suggest that residues Met<sup>758</sup> and Gln<sup>752</sup> directly bind  $P\gamma$ . A model of the PDE6 catalytic site shows that PDE6 $\alpha'$ -(750–760) forms a loop at the entrance to the cGMP-binding pocket. Binding of  $P\gamma$  to Met<sup>758</sup> would effectively block access of cGMP to the catalytic cavity, providing a structural basis for the mechanism of PDE6 inhibition.**

Photoreceptor cGMP phosphodiesterases (PDE6<sup>1</sup> family) function as effector proteins in the vertebrate visual transduction, which is mediated by the rhodopsin-coupled G protein, transducin (1–3). Retinal rod PDE6 is composed of two catalytic PDE6 $\alpha\beta$  subunits each tightly associated with the smaller inhibitory  $\gamma$  subunit ( $P\gamma$ ) (4–6). Cone PDE consists of two identical PDE $\alpha'$  subunits complexed with two copies of the cone-specific  $P\gamma$  subunit (7–9). The catalytic subunits of rod and cone PDE, as well as the respective  $P\gamma$  subunits, share a high degree of homology (9–10). The key role of  $P\gamma$  is to inhibit cGMP hydrolysis by the catalytic subunits in the dark. Upon light stimulation of photoreceptors, PDE6 is activated by GTP-bound transducin- $\alpha$ , which displaces  $P\gamma$  from the enzyme catalytic core.

\* This work was supported by National Institutes of Health Grant EY-10843. The costs of publication of this article were defrayed in part by the payment of page charges. This article must therefore be hereby marked "advertisement" in accordance with 18 U.S.C. Section 1734 solely to indicate this fact.

‡ To whom correspondence should be addressed. Tel.: 319-335-7864; Fax: 319-335-7330; E-mail: nikolai-artemyev@uiowa.edu.

<sup>1</sup> The abbreviations used are: PDE, cGMP phosphodiesterase; PDE6 $\alpha\beta$  and  $P\gamma$ ,  $\alpha$ ,  $\beta$ , and  $\gamma$  subunits of rod PDE; PDE6 $\alpha'$ ,  $\alpha'$  subunit of cone PDE; PDE5, cGMP-binding, cGMP-specific PDE (PDE5 family); PCR, polymerase chain reaction.

Two regions of  $P\gamma$  are principally involved in the interaction with the PDE6 catalytic subunits, the central polycationic region (residues 24–45 of rod  $P\gamma$ ) and the  $P\gamma$  C terminus. The C terminus of  $P\gamma$  constitutes the key inhibitory domain, whereas the polycationic region enhances the overall affinity of  $P\gamma$  toward PDE6 catalytic subunits (11–14). A cross-linking study localized the  $P\gamma$  C-terminal binding site on PDE6 $\alpha$  to residues 751–763 (residues 749–761 of PDE6 $\beta$  or PDE6 $\alpha'$ ) within the broader PDE6 catalytic domain (15). Our further analysis of the interaction between fluorescently labeled  $P\gamma$  and PDE6 $\alpha\beta$  suggests that the C terminus of  $P\gamma$  inhibits PDE6 activity by physically blocking the PDE catalytic site (16).

Progress in the investigation of the structure/function of PDE6 and the mechanism of PDE6 inhibition by  $P\gamma$  has been slowed by the lack of an efficient expression system for PDE6 (17, 18). Our approach to developing a system for PDE6 expression and mutagenesis included the construction of chimeras between PDE6 $\alpha'$  and cGMP-binding, cGMP-specific PDE (PDE5 family) (19). PDE5 and PDE6 share a common domain organization, *i.e.* two noncatalytic cGMP-binding sites located N-terminally to the conserved PDE catalytic domain (20). Furthermore, PDE5 and PDE6 display a high homology (45–48% identity) between catalytic domains, a strong substrate preference for cGMP, and similar patterns of inhibition by competitive inhibitors such as zaprinast, dipyrindamole, and sildenafil (20–23). Unlike PDE6, PDE5 is readily expressed using the baculovirus/insect cell system (24, 25). Earlier, we reported (19) the functional expression and characterization of a chimeric PDE6 $\alpha'$ /PDE5 enzyme containing the PDE6 $\alpha'$  noncatalytic cGMP-binding sites and the PDE5 catalytic domain. In this study, we generated chimeric PDE6 $\alpha'$ /PDE5 enzymes that contain the  $P\gamma$  C-terminal binding site and that are potently inhibited by  $P\gamma$ . Ala-scanning mutational analysis of the  $P\gamma$ -binding site, using chimeric PDE as a template, revealed the key interaction residues and provided structural justification for the mechanism of PDE6 inhibition.

### EXPERIMENTAL PROCEDURES

**Materials**—cGMP was obtained from Roche Molecular Biochemicals. [<sup>3</sup>H]cGMP was a product of Amersham Pharmacia Biotech. All restriction enzymes were purchased from New England Biolabs. AmpliTaq® DNA polymerase was a product of PerkinElmer Life Sciences, and *Pfu* DNA polymerase was a product of Stratagene. Rabbit polyclonal His probe (H-15) antibodies were purchased from Santa Cruz Biotechnology. Zaprinast and all other reagents were purchased from Sigma.

**Preparation of  $P\gamma$** —The  $P\gamma$  subunit was expressed in *Escherichia coli* and purified on a SP-Sepharose fast flow column and on a C-4 high pressure liquid chromatography column (Microsorb-MW, Rainin) as described (26). Purified  $P\gamma$  is lyophilized, dissolved in 20 mM HEPES buffer, pH 7.5, and stored at –80 °C until use.

**Cloning of *Chi16* and *Chi17***—The construct for expression of *Chi16* (Fig. 1) was obtained using the pFastBachHTb $\chi$ 4 vector containing cDNA coding for a PDE6 $\alpha'$ /PDE5 chimera, *Chi4* (19). A silent *SpeI* restriction site (codons for PDE5-Glu<sup>770</sup>-Leu<sup>771</sup>-Val<sup>772</sup>) was introduced into the *Chi4* cDNA using a QuikChange™ kit (Stratagene) and a pair

of complementary oligonucleotides encoding for a T  $\rightarrow$  A substitution. The pFastBacHTbChi4 plasmid was used as a template for PCR using a *Pfu* DNA polymerase. The PCR product was digested with *Dpn*I-specific for methylated and hemimethylated DNA and transformed into *E. coli* DH5 $\alpha$ . To generate Chi16, the PDE6 $\alpha'$  DNA fragment coding for PDE6 $\alpha'$ -(737–784) was PCR-amplified using a pBlueScriptPDE6 $\alpha'$  vector (8, 19) as a template. The PCR product was cut with *Spe*I and *Stu*I and ligated into the *Spe*I/*Stu*I-digested pFastBacHTbChi4-*Spe*I. To obtain Chi17, the *Pvu*II/*Sph*I fragment from pFastBacHTbChi16 was subcloned into pFastBacHTbPDE5 (19).

**Site-directed Mutagenesis of Chi16**—A unique *Nhe*I site was introduced into Chi16 cDNA using a QuikChange<sup>TM</sup> kit (Stratagene). Single amino acid substitutions corresponding to PDE6 $\alpha'$  residues at positions 750–760 were generated in Chi16 by PCR-directed mutagenesis. To facilitate the screening procedure, mutant primers were designed to either introduce or eliminate a suitable restriction site. For each mutant, the PCR product was obtained using a forward primer containing a mutated codon and a reverse primer carrying the *Stu*I site. Purified PCR products were used as reversed primers for a second round PCR amplification with a forward primer containing *Nhe*I. The pFastBacHTbChi16 vector was used as a template in both PCR rounds. Final PCR products were digested with *Nhe*I/*Stu*I and subcloned into the pFastBacHTbChi16 vector cut with the same enzymes. Sequences of all mutants were verified by automated DNA sequencing at the University of Iowa DNA Core Facility.

**Expression and Purification of Chi16, Chi17, and Chi16 Mutants**—Sf9 cells were harvested at 60 h after infection, washed with 20 mM Tris-HCl buffer, pH 7.8, containing 50 mM NaCl, and resuspended in the same buffer containing a protease inhibitor mixture (10  $\mu$ g/ml pepstatin, 5  $\mu$ g/ml leupeptin, and 0.2 mM phenylmethylsulfonyl fluoride). After sonication using 30-s pulses for a total duration of 3 min, the supernatant (100,000  $\times$  g, 45 min) was loaded onto a column with a His-Bind resin (Novagen) equilibrated with 20 mM Tris-HCl buffer, pH 7.8, containing 10 mM imidazole. The resin was washed with a 5 $\times$  volume of the same buffer containing 500 mM NaCl and 25 mM imidazole. Proteins were eluted with the buffer containing 250 mM imidazole.  $\beta$ -Mercaptoethanol (2 mM) was added to the mixture. Purified proteins were dialyzed against 40% glycerol and stored at  $-20^\circ\text{C}$ .

**Other Methods**—PDE activity was measured using [<sup>3</sup>H]cGMP as described (27, 28). Less than 15% of cGMP was hydrolyzed during these reactions. The  $K_i$  values for inhibition of PDE activity by  $\text{P}\gamma$  and zaprinast were measured using 0.5  $\mu\text{M}$  cGMP (*i.e.* <35% of  $K_m$  value for chimeric and mutant PDEs). Protein concentrations were determined by the method of Bradford (29), using IgG as a standard, or by using calculated extinction coefficients at 280 nm. The molar concentrations of Chi16 and mutant PDEs, [PDE], were calculated based on the fraction of PDE protein in preparations and the molecular mass of 93.0 kDa. The fractional concentrations of PDE were determined from analysis of the Coomassie Blue-stained SDS gels using a Hewlett-Packard ScanJet II CX/T scanner and Scion Image Beta 4.02 software. A typical fraction of PDE in partially purified preparations was 10–15%. The  $k_{\text{cat}}$  values for cGMP hydrolysis were calculated as  $V_{\text{max}}/[\text{PDE}]$ . SDS-polyacrylamide gel electrophoresis was performed by the method of Laemmli (30) in 10–12% acrylamide gels. For Western immunoblotting, proteins were transferred to nitrocellulose (0.1  $\mu\text{m}$ , Schleicher & Schuell) and analyzed using rabbit His probe (H-15) or sheep anti-PDE6 $\alpha'$  antibodies (19, 31). The antibody-antigen complexes were detected using anti-rabbit or anti-goat/sheep IgG conjugated to horseradish peroxidase and ECL reagent (Amersham Pharmacia Biotech). Fitting the experimental data to equations was performed with nonlinear least squares criteria using GraphPad Prizm Software. The  $K_i$ ,  $K_m$ , and  $\text{IC}_{50}$  values are expressed as mean  $\pm$  S.E. for three independent measurements.

## RESULTS

**Functional Analysis of Chimeric PDE6 $\alpha'$ /PDE5 Proteins Containing the  $\text{P}\gamma$ -binding Site**—Previously we demonstrated (19) a functional expression of chimeric PDE6 $\alpha'$ /PDE5 protein, Chi4, using Baculovirus/Sf9 system. Chi4 contained the regulatory, noncatalytic cGMP-binding domain of PDE6 $\alpha'$  and the catalytic domain of PDE5 (Fig. 1A). Chi4 was used as a basic template for the generation of new chimeras in which various portions of the PDE5 catalytic domain were replaced by corresponding sequences from PDE6 $\alpha'$ . Chi16, containing a segment of 48 residues from PDE6 $\alpha'$  (PDE6 $\alpha'$ -(737–784)) (Fig. 1), was functionally expressed in Sf9 cells with a yield of soluble protein at  $\sim$ 100  $\mu\text{g}/100$  ml of culture. Chi16 hydrolyzed cGMP

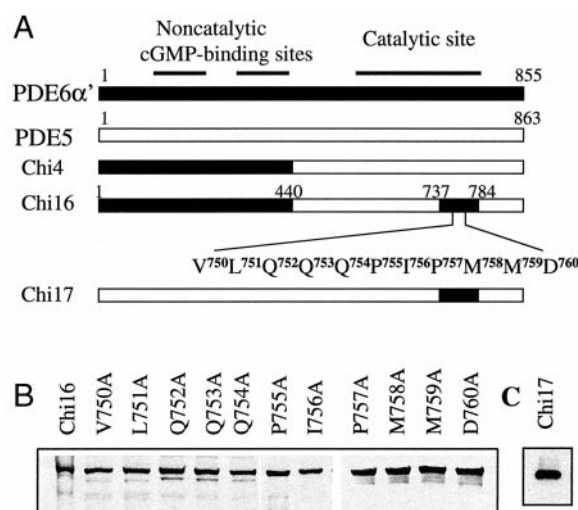


FIG. 1. A, schematic representation of PDE6 $\alpha'$ /PDE5 chimeras. Shown are the residues in the  $\text{P}\gamma$ -binding site substituted by alanine. B, Western blot analysis of Chi16, Chi17, and Chi16 mutants. Recombinant His<sub>6</sub>-tagged chimeras and mutants were expressed in Sf9 cells and partially purified using chromatography on a His-Bind resin (Novagen) as described under "Experimental Procedures." Immunoblotting of Chi16 and Chi16 mutants (B) was performed using sheep anti-PDE6 $\alpha'$  antibodies (19). Chi17 (C) was detected using rabbit polyclonal His probe (H-15) antibodies.

with a  $K_m$  value of 2.8  $\mu\text{M}$  and a  $k_{\text{cat}}$  value of 9.0  $\text{s}^{-1}$  (Fig. 2A and Table I). Both kinetic parameters of Chi16 were comparable to those of PDE5 and Chi4 (Table I). In addition, Chi16 was potently inhibited by zaprinast, a PDE5/PDE6-specific competitive inhibitor ( $\text{IC}_{50}$  0.12  $\mu\text{M}$ ) (Fig. 2B).

The PDE6 $\alpha'$ -(737–784) insert includes a segment PDE6 $\alpha'$ -(749–761) that was previously identified as a binding site for the  $\text{P}\gamma$  C terminus. The sequence corresponding to PDE6 $\alpha'$ -(749–761) is unique for photoreceptor PDEs, which show a strong conservation at this site (15). In contrast to PDE5 and Chi4 (19), the catalytic activity of Chi16 was effectively inhibited by  $\text{P}\gamma$ . The  $K_i$  value of 3.6 nM indicates that  $\text{P}\gamma$  binds to Chi16 with only a 20-fold lower affinity than the affinity of its interaction with native PDE6 $\alpha'$  (Fig. 3 and Table I).

To test the potential role of the PDE6 noncatalytic cGMP-binding domain, the PDE6 $\alpha'$ -(737–784) region was also replaced into the PDE5 cDNA (Fig. 1). The resulting chimera, Chi17, had catalytic properties similar to those of PDE5 and Chi16 ( $K_m$  1.9  $\mu\text{M}$  and  $k_{\text{cat}}$  9.8  $\text{s}^{-1}$ ) (Fig. 2A and Table I). The  $\text{IC}_{50}$  value for the Chi17 inhibition by zaprinast (0.77  $\mu\text{M}$ ) was similar to the  $\text{IC}_{50}$  value for PDE5 but somewhat higher than the  $\text{IC}_{50}$  value for Chi16 (Fig. 2B and Table I).  $\text{P}\gamma$  inhibited the cGMP hydrolysis by Chi17 less potently than the catalytic activity of Chi16. The maximal inhibition was up to 70% of Chi17 activity, and the  $K_i$  value was 142 nM (Fig. 3). These results suggest that the noncatalytic cGMP-binding domain of PDE6 $\alpha'$  contributes to the high affinity interaction with  $\text{P}\gamma$ .

**Ala-scanning Mutagenesis of the  $\text{P}\gamma$ -binding Region**—An Ala-scanning mutagenesis of the  $\text{P}\gamma$  C-terminal binding site in Chi16 was performed to identify the  $\text{P}\gamma$ -binding residues of PDE6 $\alpha'$ . Eleven consecutive residues starting at position 750 were substituted with alanine. The Chi16 mutants were expressed in Sf9 cells and partially purified from the soluble fraction using an affinity chromatography on a His-Bind resin. The expression levels of soluble Chi16 mutants were 50–100  $\mu\text{g}/100$  ml culture, *i.e.* comparable to that of Chi16. All Chi16 mutants were analyzed for their ability to hydrolyze cGMP. Two mutants, L751A and D760A, were catalytically inactive. Two other mutants, P755A and I756A, displayed notably reduced catalytic rates (Table I). In addition to lowering the  $k_{\text{cat}}$

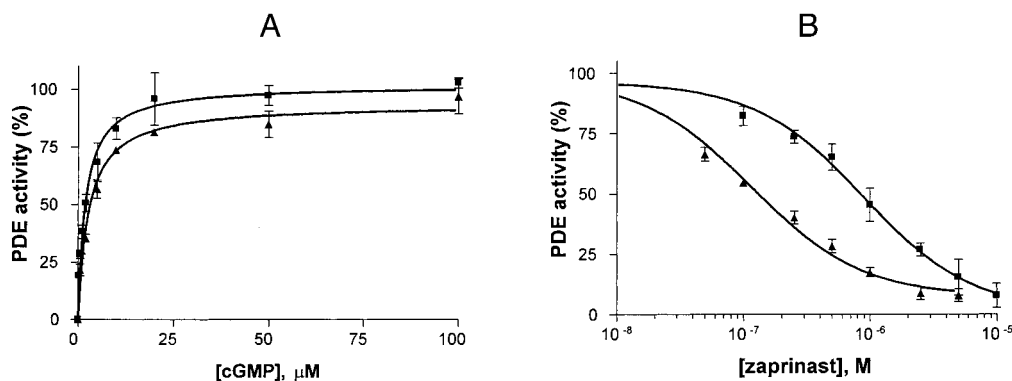


FIG. 2. **Catalytic properties of Chi16 and Chi17.** *A*, kinetics of cGMP hydrolysis by Chi16 (▲) and Chi17 (■). PDE activities were determined using 0.1  $\mu\text{Ci}$  of [ $^3\text{H}$ ]cGMP and increasing concentrations of unlabeled cGMP. The rates of cGMP hydrolysis are expressed as percentage of maximal activity of PDE5 (9.6 mol of cGMP·mol PDE $^{-1}$ ·s $^{-1}$ ) (19). The kinetic characteristics for Chi16 ( $K_m$ ,  $2.8 \pm 0.5 \mu\text{M}$ ,  $k_{\text{cat}}$   $9.0 \text{ s}^{-1}$ ) and Chi 17 ( $K_m$   $1.9 \pm 0.3 \mu\text{M}$ ,  $k_{\text{cat}}$   $9.8 \text{ s}^{-1}$ ) were calculated from the fitting curves. *B*, inhibition of Chi16 and Chi17 activity by zaprinast. Activities of Chi16 (▲) and Chi17 (■) were determined in the presence of 0.5  $\mu\text{M}$  cGMP and increasing concentrations of zaprinast and were expressed as a percentage of respective PDE activity in the absence of zaprinast. The calculated  $\text{IC}_{50}$  values for Chi16 and Chi17 were  $0.12 \pm 0.01$  and  $0.77 \pm 0.02 \mu\text{M}$ , respectively.

TABLE I  
Functional properties of Chi16 mutants

| Mutant                      | $K_m$           | $k_{\text{cat}}$ | $\text{IC}_{50}$ for zaprinast | $K_i$ for $\text{P}\gamma$ |
|-----------------------------|-----------------|------------------|--------------------------------|----------------------------|
|                             | $\mu\text{M}$   | $\text{s}^{-1}$  | $\mu\text{M}$                  | $\text{nM}$                |
| PDE6 $\alpha'$ <sup>a</sup> | $23 \pm 2$      | 3500             | $0.28 \pm 0.05$                | $0.17 \pm 0.02$            |
| PDE5 <sup>a</sup>           | $3.0 \pm 0.5$   | 9.6              | $0.75 \pm 0.07$                | NA                         |
| Chi4 <sup>a</sup>           | $1.5 \pm 0.3$   | 10.0             | $0.65 \pm 0.04$                | NA                         |
| Chi16                       | $2.8 \pm 0.5$   | 9.0              | $0.12 \pm 0.01$                | $3.6 \pm 0.4$              |
| Chi17                       | $1.9 \pm 0.3$   | 9.8              | $0.77 \pm 0.02$                | $142 \pm 13$               |
| V750A                       | $8.7 \pm 0.9$   | 4.8              | $0.40 \pm 0.01$                | $0.78 \pm 0.05$            |
| L751A                       | NA <sup>b</sup> | NA               | NA                             | NA                         |
| Q752A                       | $12 \pm 2$      | 8.0              | $0.20 \pm 0.01$                | $29 \pm 4$                 |
| Q753A                       | $7.3 \pm 0.8$   | 9.5              | $0.27 \pm 0.04$                | $4.2 \pm 0.7$              |
| Q754A                       | $11 \pm 1$      | 7.3              | $0.15 \pm 0.01$                | $2.1 \pm 0.4$              |
| P755A                       | $42 \pm 6$      | 0.8              | $0.19 \pm 0.01$                | $0.72 \pm 0.1$             |
| I756A                       | $4.6 \pm 0.8$   | 1.4              | $0.27 \pm 0.03$                | $2.3 \pm 0.3$              |
| P757A                       | $15 \pm 2$      | 9.0              | $0.18 \pm 0.01$                | $4.1 \pm 0.5$              |
| M758A                       | $9.5 \pm 0.9$   | 8.9              | $0.26 \pm 0.01$                | $97 \pm 10$                |
| M759A                       | $7.9 \pm 0.6$   | 6.8              | $0.23 \pm 0.02$                | $5.1 \pm 0.4$              |
| D760A                       | NA              | NA               | NA                             | NA                         |

<sup>a</sup> Data from Granovsky *et al.* (19).

<sup>b</sup> NA, not applicable.

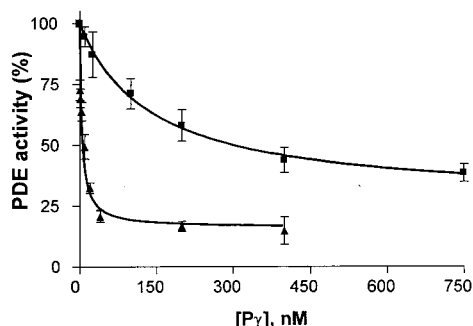


FIG. 3. **Inhibition of the catalytic activity of Chi16 and Chi17 by  $\text{P}\gamma$ .** The activities of Chi16 (▲) and Chi17 (■) were determined upon addition of increasing concentrations of  $\text{P}\gamma$ , using 0.5  $\mu\text{M}$  cGMP as a substrate. The  $K_i$  values from the inhibition curves were  $3.6 \pm 0.4 \text{ nM}$  for Chi16 and  $142 \pm 13 \text{ nM}$  for Chi17.

value for cGMP hydrolysis, the P755A substitution also resulted in an increase in the  $K_m$  value from 2.8 to 42  $\mu\text{M}$  (Table I). The catalytic properties of P755A indicate that this mutation likely affected the overall folding of the catalytic site in Chi16. The  $K_m$  values for cGMP hydrolysis for the remaining Chi16 mutants were within the 4–15  $\mu\text{M}$  range (Table I). Inhibition of Chi16 mutants by zaprinast revealed no large variations in their  $\text{IC}_{50}$  values, which were comparable to the  $\text{IC}_{50}$  value for Chi16 (Table I).

Next, all catalytically active Chi16 mutants were examined for inhibition by  $\text{P}\gamma$ . Most of the mutants retained a functional interaction with  $\text{P}\gamma$  with the  $K_i$  values of  $\sim 0.8$  to 5  $\text{nM}$  (Table I). Two mutants, Q752A and M758A, were defective in  $\text{P}\gamma$  binding. The Q752A mutation had a moderate effect on interaction with  $\text{P}\gamma$ .  $\text{P}\gamma$  was capable of full inhibition of the Q752A catalytic activity, but the  $K_i$  value was increased to 29  $\text{nM}$  (Fig. 4C). A major impairment of the  $\text{P}\gamma$  interaction was observed for the M758A mutant. The inhibition of M758A by  $\text{P}\gamma$  was incomplete ( $\sim 75\%$ ) with the  $K_i$  value of 97  $\text{nM}$  (Fig. 4C). Since the catalytic properties of Q752A and M758A were similar to those of Chi16 (Fig. 4), the defects of  $\text{P}\gamma$  binding are not likely to be caused by alterations in overall folding of the catalytic domain in these mutants.

#### DISCUSSION

The vertebrate visual transduction cascade is among the most studied and best understood G protein signaling systems. Yet, PDE6, the key enzyme of vision, remains arguably one of the most obscure G protein effectors in terms of understanding its structure/function relationship. Difficulties in the development of an efficient expression system for PDE6 have precluded the systematic mutational analysis of the enzyme (17–19). Our attempts to express functionally wild-type PDE6 $\alpha'$  and co-express PDE6 $\alpha'$  with  $\text{P}\gamma$  using the Baculovirus/Sf9, COS7, or retinoblastoma Y79 cell systems have also been unsuccessful.<sup>2</sup> A construction of chimeric enzymes between PDE6 $\alpha'$  and related PDE5 has been proven as a useful tool for the study of PDE6. Previously, we demonstrated that a fully functional chimeric PDE6 $\alpha'$ /PDE5 enzyme, containing the PDE6 $\alpha'$  noncatalytic cGMP-binding sites and the PDE5 catalytic domain, can be efficiently expressed in the Baculovirus/insect cell system (19). This chimeric enzyme showed catalytic properties and noncatalytic cGMP-binding characteristics analogous to those of PDE5 and PDE6 $\alpha'$ , respectively. Chimeric PDE6 $\alpha'$ /PDE5 proteins containing the PDE6 $\alpha'$ -active site were catalytically inactive, suggesting that the catalytic domain contains specific sequences preventing its functional folding in insect cells. Based on these findings, we generated and analyzed a number of chimeric PDE6 $\alpha'$ /PDE5 proteins with replacements of various PDE5 catalytic domain segments by corresponding PDE6 $\alpha'$  sequences. A sequence, PDE6 $\alpha'$ -(737–784), containing the  $\text{P}\gamma$  C-terminal binding site  $\text{P}\alpha'$ -(749–761) (15), has been introduced in one of these chimeras, Chi16 (Fig. 1). Not only was Chi16 catalytically active with  $K_m$  and

<sup>2</sup> A. E. Granovsky and N. O. Artemyev, unpublished observations.



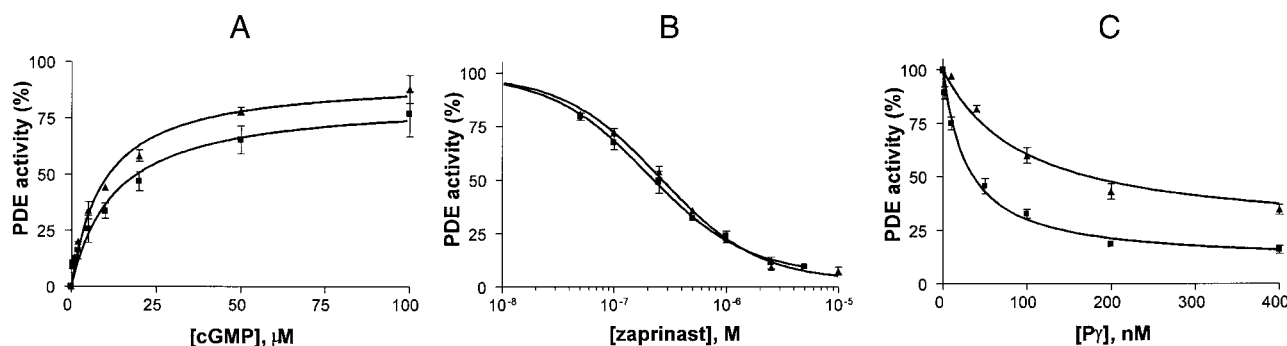
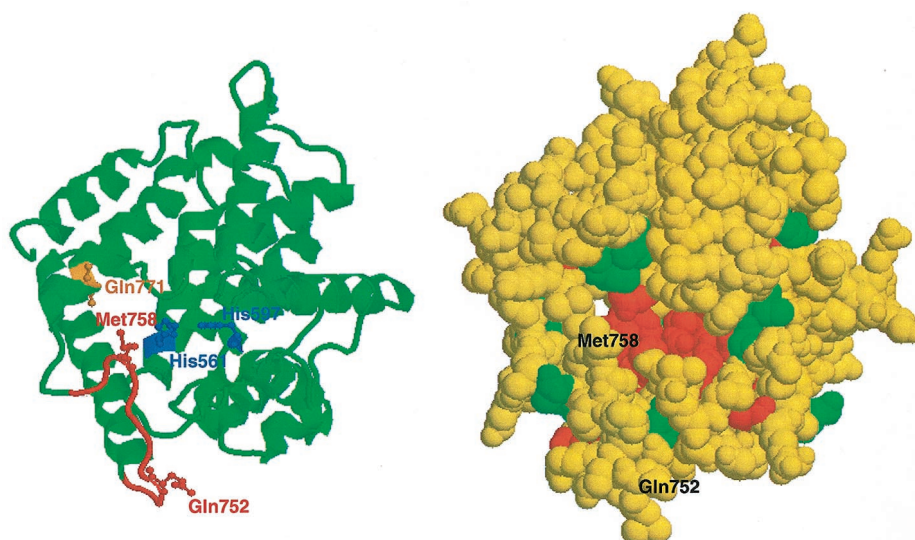


FIG. 4. **Functional properties of Chi16 mutants, Q752A and M758A.** *A*, kinetics of cGMP hydrolysis by Q752A (■) and M758A (▲). PDE activities were determined using 0.1  $\mu\text{Ci}$  of [ $^3\text{H}$ ]cGMP and increasing concentrations of unlabeled cGMP. The rates of cGMP hydrolysis are expressed as percentage of maximal activity of PDE5 (9.6 mol of cGMP·mol PDE $^{-1}$ ·s $^{-1}$ ) (19). The kinetic characteristics for Q752A ( $K_m$  12  $\pm$  2  $\mu\text{M}$ ,  $k_{\text{cat}}$  8.0 s $^{-1}$ ) and M758A ( $K_m$  9.5  $\pm$  0.9  $\mu\text{M}$ ,  $k_{\text{cat}}$  8.9 s $^{-1}$ ) were calculated from the fitting curves. *B*, inhibition of Q752A and M758A activity by zaprinast. Activities of Q752A (■) and M758A (▲) were determined in the presence of 0.5  $\mu\text{M}$  cGMP and increasing concentrations of zaprinast. The activities were expressed as a percentage of respective PDE activity in the absence of zaprinast. The calculated  $\text{IC}_{50}$  values for Q752A and M758A were 0.20  $\pm$  0.01 and 0.26  $\pm$  0.01  $\mu\text{M}$ , respectively. *C*, inhibition of the catalytic activity of Q752A and M758A by P $\gamma$ . The activities of Q752A (■) and M758A (▲) were determined upon addition of increasing concentrations of P $\gamma$ , using 0.5  $\mu\text{M}$  cGMP as a substrate. The  $K_i$  values from the inhibition curves were 29  $\pm$  4 nM for Q752A and 97  $\pm$  10 nM for M758A.

FIG. 5. **A model of the PDE6 $\alpha'$  catalytic domain.** *Left*, the model was generated with the Swiss-PdbViewer (40) using the coordinates of the PDE4 structure as a template (36). The P $\gamma$  C-terminal binding site, P $\gamma$ (749–761) (15), is shown in red. The P $\gamma$  contact residues, Gln $^{752}$  and Met $^{758}$  (red), the key catalytic metal-binding residues, His $^{561}$  and His $^{597}$  (blue), and the cGMP guanine ring binding residue, Gln $^{771}$  (orange) are shown in “ball-and-stick” representation. The image was obtained using RasMol (version 2.6). *Right*, a space-filling representation of the model, orientated as *left*, with residues colored by multiple sequence alignment, was generated using Protein Explorer 1.485 Beta. The multiple sequence alignment CLUSTALW included PDEs from eight PDE families, PDE1–6, -10, and -11. Identical residues are red, similar residues are green, and different residues are yellow.



$k_{\text{cat}}$  values similar to PDE5, but it also acquired sensitivity to P $\gamma$ . The  $K_i$  value of Chi16 for P $\gamma$  (3.6 nM) was just 10–20-fold higher than the  $K_i$  values of native PDE6 $\alpha'$  reported previously (19, 32). Contacts between P $\gamma$  and the PDE6 $\alpha'$  catalytic domain outside of PDE6 $\alpha'$ -(737–784) may account for the lower  $K_i$  value of the native enzyme. The noncatalytic cGMP-binding sites are allosterically coupled with the P $\gamma$ -binding sites and may regulate P $\gamma$  affinity for the PDE catalytic subunits (33–35). To test the role of the cGMP-binding domain, PDE6 $\alpha'$ -(737–784) was also replaced into the wild-type PDE5 sequence (Chi17). P $\gamma$  inhibited Chi17 ( $K_i$  of 142 nM) less potently than Chi16, indicating that the noncatalytic cGMP-binding domain of PDE6 $\alpha'$ , allosterically or due to additional contacts, enhances the P $\gamma$  interaction with the catalytic domain.

Previously we demonstrated (16) that binding of the P $\gamma$  C terminus to the PDE6 catalytic domain blocks the access of cGMP to the catalytic site. The P $\gamma$  C-terminal binding was also competitive with zaprinast. We concluded that residues that participate in the binding/hydrolysis of cGMP and the binding of competitive inhibitors are in a very close proximity to the P $\gamma$  C-terminal binding residues in a three-dimensional structure of PDE6 (16). In this study, an introduction of the P $\gamma$ -binding site into the PDE5 catalytic domain did not appreciably alter the catalytic properties. Therefore, the residues that bind P $\gamma$

are not directly involved in binding/hydrolysis of cGMP by PDE6, and they likely form a domain distinct from the catalytic pocket. Both conclusions, proximity of the P $\gamma$ -site to and its structural independence from the catalytic pocket, are supported by the model of PDE6 catalytic site (Fig. 5). The model was generated based on the recently determined structure of PDE4 catalytic domain, the first crystal structure of a PDE enzyme (36). According to this model, the P $\gamma$ -binding site, PDE6 $\alpha'$ -(749–761), forms a loop near the entrance to the catalytic cGMP-binding pocket. However, PDE6 $\alpha'$ -(749–761) residues do not participate in the formation of the catalytic cavity itself. The latter is primarily assembled by residues conserved in the PDE superfamily. These residues include two histidines, His $^{561}$  and His $^{597}$  (His $^{238}$  and His $^{274}$  in PDE4), critical for coordination of two metal ions (36) (Fig. 5). The two metal atoms, apparently a tightly bound Zn $^{2+}$  and a more loosely associated Mg $^{2+}$ , are central to the hydrolysis of cyclic nucleotides by PDE6 (37). Corresponding residues, His $^{607}$  and His $^{643}$ , are necessary for the metal support of catalysis in PDE5 (38). Another important residue within the PDE6 $\alpha'$  catalytic pocket is conserved Gln $^{771}$  (Fig. 5). The docking of cAMP into the PDE4 structure shows that a side chain of an analogous Gln $^{443}$  hydrogen bonds with the 1-N and 6-NH $_2$  groups of the adenine base, but if the Gln $^{443}$  amide group is rotated by 180° it may

interact with the 1-NH and 6-CO groups of cGMP (36). Gln<sup>443</sup> in PDE4 is constrained by the interaction with Tyr<sup>403</sup> (36). The Tyr residue is substituted by Gln<sup>729</sup> and Gln<sup>765</sup> in PDE6 and PDE5, respectively, which appears to contribute to the cGMP substrate specificity. The Gln<sup>765</sup> → Tyr substitution was among several mutations that shifted the cGMP/cAMP selectivity of PDE5 (39).

Ala-scanning mutational analysis of PDE6 $\alpha'$ -(750–760) in Chi16 identified two mutants, Q752A and M758A, with impaired inhibition by P $\gamma$ . The M758A substitution resulted in a particularly profound defect of P $\gamma$  binding. Both mutants retained the catalytic properties ( $K_m$  and  $k_{cat}$ ) for cGMP hydrolysis and the IC<sub>50</sub> values for inhibition by zaprinast similar to those of Chi16, suggesting their intact overall folding. The model of the PDE6 $\alpha'$  catalytic domain shows that the side chains of Gln<sup>752</sup> and Met<sup>758</sup> are solvent-exposed and are similarly orientated on the surface of the molecule. Hence, in all probability, these residues directly interact with P $\gamma$ . If the P $\gamma$ C terminus is lined up along the plane formed by the side chains of Gln<sup>752</sup> and Met<sup>758</sup>, it may also make a contact with Pro<sup>755</sup>. Our data do not rule out the possibility of this contact. The P755A mutant had a significantly reduced rate of cGMP hydrolysis, and therefore, its inhibition by P $\gamma$  might not be directly compared with that for Chi16. Out of the residues, Met<sup>758</sup> is located at the very tip of the P $\gamma$ -binding loop facing the opening of the catalytic cavity. Such a location of the P $\gamma$ -binding residue would allow P $\gamma$  to effectively block the entry of cGMP into the catalytic pocket.

**Acknowledgment**—The services provided by the Diabetes and Endocrinology Research Center of the University of Iowa were supported by National Institutes of Health Grant DK-25295.

## REFERENCES

- Chabre, M., and Deterre, P. (1989) *Eur. J. Biochem.* **179**, 255–266
- Yarfitz, S., and Hurley, J. B. (1994) *J. Biol. Chem.* **269**, 14329–14332
- Beavo, J. A. (1995) *Physiol. Rev.* **75**, 725–748
- Baehr, W., Devlin, M. J., and Applebury, M. L. (1979) *J. Biol. Chem.* **254**, 11669–11677
- Hurley, J. B., and Stryer, L. (1982) *J. Biol. Chem.* **257**, 11094–11099
- Deterre, P., Bigay, J., Forquet, F., Robert, M., and Chabre, M. (1988) *Proc. Natl. Acad. Sci. U. S. A.* **85**, 2424–2428
- Gillespie, P. G., and Beavo, J. A. (1988) *J. Biol. Chem.* **263**, 8133–8141
- Li, T., Volpp, K., and Applebury, M. L. (1990) *Proc. Natl. Acad. Sci. U. S. A.* **87**, 293–297
- Hamilton, S. E., and Hurley, J. B. (1990) *J. Biol. Chem.* **265**, 11259–11264
- Lipkin, V. M., Khrantsov, N. V., Vasilevskaya, N. V., Atabekova, K. G., Muradov, K. G., Li, T., Johnston, J. P., Volpp, K. J., and Applebury, M. L. (1990) *J. Biol. Chem.* **265**, 12955–12959
- Artemyev, N. O., and Hamm, H. E. (1992) *Biochem. J.* **283**, 273–279
- Takemoto, D. J., Hurt, D., Oppert, B., and Cunnick, J. (1992) *Biochem. J.* **281**, 637–643
- Brown, R. L. (1992) *Biochemistry* **31**, 5918–5925
- Skiba, N. P., Artemyev, N. O., and Hamm, H. E. (1995) *J. Biol. Chem.* **270**, 13210–13215
- Artemyev, N. O., Natochin, M., Busman, M., Schey, K. L., and Hamm, H. E. (1996) *Proc. Natl. Acad. Sci. U. S. A.* **93**, 5407–5412
- Granovsky, A. E., Natochin, M., and Artemyev, N. O. (1997) *J. Biol. Chem.* **272**, 11686–11689
- Piriev, N. I., Yamashita, C., Samuel, G., and Farber, D. (1993) *Proc. Natl. Acad. Sci. U. S. A.* **90**, 9340–9344
- Qin, N., and Baehr, W. (1994) *J. Biol. Chem.* **269**, 3265–3271
- Granovsky, A. E., Natochin, M., McEntaffer, R. L., Haik, T. L., Francis, S. H., Corbin, J. D., and Artemyev, N. O. (1998) *J. Biol. Chem.* **273**, 24485–24490
- McAllister-Lucas, L. M., Sonnenburg, W. K., Kadlecak, A., Seger, D., Trong, H. L., Colbran, J. L., Thomas M. K., Walsh, K. A., Francis, S. H., Corbin, J. D., and Beavo, J. A. (1993) *J. Biol. Chem.* **268**, 22863–22873
- Gillespie, P. G., and Beavo, J. A. (1989) *Mol. Pharmacol.* **36**, 773–781
- Turko, I. V., Ballard, S. A., Francis, S. H., and Corbin, J. D. (1999) *Mol. Pharmacol.* **56**, 124–130
- Ballard, S. A., Gingell, C. J., Tang, K., Turner, L. A., Price, M. E., and Naylor, A. M. (1998) *J. Urol.* **159**, 2164–2171
- Turko, I. V., Haik, T. L., McAllister-Lucas, L. M., Burns, F., Francis, S. H., and Corbin, J. D. (1996) *J. Biol. Chem.* **271**, 22240–22244
- Turko, I. V., Francis, S. H., and Corbin, J. D. (1998) *J. Biol. Chem.* **273**, 6460–6466
- Artemyev, N. O., Arshavsky, V. Y., and Cote, R. H. (1998) *Methods* **14**, 93–104
- Thompson, W. J., and Appleman, M. M. (1971) *Biochemistry* **10**, 311–316
- Natochin, M., and Artemyev, N. O. (2000) *Methods Enzymol.* **315**, 539–554
- Bradford, M. M. (1976) *Anal. Biochem.* **72**, 248–254
- Laemmli, U. K. (1970) *Nature* **227**, 680–685
- Towbin, H., Staehelin, T., and Gordon, J. (1979) *Proc. Natl. Acad. Sci. U. S. A.* **76**, 4350–4354
- Hamilton, S. E., Prusti, R. K., Bentley, J. K., Beavo, J. A., and Hurley, J. B. (1993) *FEBS Lett.* **318**, 157–161
- Yamazaki, A., Bartucca, F., Ting, A., and Bitensky, M. W. (1982) *Proc. Natl. Acad. Sci. U. S. A.* **79**, 3702–3706
- Cote, R. H., Bownds, M. D., and Arshavsky, V. Y. (1994) *Proc. Natl. Acad. Sci. U. S. A.* **91**, 4845–4849
- Mou, H., Grazio, H. J., Cook, T. A., Beavo, J. A., and Cote, R. H. (1999) *J. Biol. Chem.* **274**, 18813–18820
- Xu, R. X., Hassell, A. M., Vanderwall, D., Lambert, M. H., Holmes, W. D., Luther, M. A., Rocque, W. J., Milburn, M. V., Zhao, Y., Ke, H., and Nolte, R. T. (2000) *Science* **288**, 1822–1825
- He, F., Seryshev, A. B., Cowan, C. W., and Wensel, T. G. (2000) *J. Biol. Chem.* **275**, 20572–20577
- Francis, S. H., Turko, I. V., Grimes, K. A., and Corbin, J. D. (2000) *Biochemistry* **39**, 9591–9596
- Turko, I. V., Francis, S. H., and Corbin, J. D. (1998) *Biochemistry* **37**, 4200–4205
- Guex, N., and Peitsch, M. C. (1997) *Electrophoresis* **18**, 2714–2723

**Identification of the  $\gamma$  Subunit-interacting Residues on Photoreceptor cGMP  
Phosphodiesterase, PDE6  $\alpha'$**

Alexey E. Granovsky and Nikolai O. Artemyev

*J. Biol. Chem.* 2000, 275:41258-41262.

doi: 10.1074/jbc.M008094200 originally published online October 6, 2000

---

Access the most updated version of this article at doi: [10.1074/jbc.M008094200](https://doi.org/10.1074/jbc.M008094200)

Alerts:

- [When this article is cited](#)
- [When a correction for this article is posted](#)

[Click here](#) to choose from all of JBC's e-mail alerts

This article cites 40 references, 27 of which can be accessed free at <http://www.jbc.org/content/275/52/41258.full.html#ref-list-1>